Heliyon 10 (2024) e27165

Contents lists available at ScienceDirect

Heliyon

journal homepage: www.cell.com/heliyon

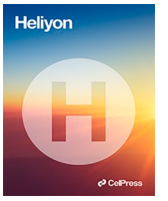

Research article

Combining WGCNA and machine learning to identify mechanisms and biomarkers of ischemic heart failure development after acute myocardial infarction

Yan Li [a,b], Ying Hu [b], Feng Jiang [b], Haoyu Chen [b], Yitao Xue [b,**], Yiding Yu [a,*]

[a] Shandong University of Traditional Chinese Medicine, Jinan, 250014, China
[b] Affiliated Hospital of Shandong University of Traditional Chinese Medicine, Jinan, 250014, China

ARTICLE INFO

Keywords:
Ischemic heart failure
Acute myocardial infarction
Machine learning
Immune infiltration analysis
Bioinformatics

ABSTRACT

Background: Ischemic heart failure (IHF) is a serious complication after acute myocardial infarction (AMI). Understanding the mechanism of IHF after AMI will help us conduct early diagnosis and treatment.
Methods: We obtained the AMI dataset GSE66360 and the IHF dataset GSE57338 from the GEO database, and screened overlapping genes common to both diseases through WGCNA analysis. Subsequently, we performed GO and KEGG enrichment analysis on overlapping genes to elucidate the common mechanism of AMI and IHF. Machine learning algorithms are also used to identify key biomarkers. Finally, we performed immune cell infiltration analysis on the dataset to further evaluate immune cell changes in AMI and IHF.
Results: We obtained 74 overlapping genes of AMI and IHF through WGCNA analysis, and the enrichment analysis results mainly focused on immune and inflammation-related mechanisms. Through the three machine learning algorithms of LASSO, RF and SVM-RFE, we finally obtained the four Hub genes of IL1B, TIMP2, IFIT3, and P2RY2, and verified them in the IHF dataset GSE116250, and the diagnostic model AUC = 0.907. The results of immune infiltration analysis showed that 8 types of immune cells were significantly different in AMI samples, and 6 types of immune cells were significantly different in IHF samples.
Conclusion: We explored the mechanism of IHF after AMI by WGCNA, enrichment analysis, and immune infiltration analysis. Four potential diagnostic candidate genes and therapeutic targets were identified by machine learning algorithms. This provides a new idea for the pathogenesis, diagnosis, and treatment of IHF after AMI.

1. Introduction

Acute myocardial infarction (AMI) is a severe heart attack caused by coronary occlusion and characterized by myocardial necrosis caused by exposure of the myocardium supplied by the occluded coronary artery to an ischemic environment [1]. With the development of interventional techniques and drugs, the survival rate of patients with AMI has continuously improved, but the incidence of complications has also increased [2]. Among them, ischemic heart failure (IHF) is the most serious complication after myocardial

* Corresponding author.
** Corresponding author.
E-mail addresses: xytsdzydfy@126.com (Y. Xue), 1078607526@qq.com (Y. Yu).

https://doi.org/10.1016/j.heliyon.2024.e27165
Received 10 July 2023; Received in revised form 15 January 2024; Accepted 26 February 2024
Available online 27 February 2024

infarction, with an estimated 1-year incidence rate of 23.4% [3]. IHF after AMI has become a major public health problem because of its morbidity, mortality, readmission rates, and medical expenditures [4].

The progression of IHF after AMI is multifactorial, mainly depending on the degree of myocardial injury, reperfusion injury, myocardial dormancy, ventricular remodeling, and neuroendocrine stimulation [5]. A more comprehensive understanding of the mechanisms of IHF after AMI will allow us to identify patients with acute AMI at risk for IHF and to intervene early to reduce the socioeconomic burden. Previous studies have shown that conventional biomarkers B-type natriuretic peptide or N-terminal probrain natriuretic peptide, as well as troponin I and C-reactive protein can aid in the detection of the development of IHF after AMI. But these biomarkers are also elevated in other diseases, such as renal impairment or thyroid disease, which means they are less specific [6–8]. In addition, these biomarkers cannot reflect the pathological mechanism of IHF after AMI, and cannot provide a reference for the screening of therapeutic targets. Therefore, we still need to identify new biomarkers and potential therapeutic targets.

The rapid development of high-throughput technology and bioinformatics can help us screen for biomarkers and therapeutic targets. Previous bioinformatics studies mainly identified available biomarkers through differential gene and PPI network analysis [9, 10]. However, these studies ignored the common high-correlation gene clusters between AMI and IHF, and the accuracy of PPI network analysis was also questioned [11]. With the development of analysis methods, weighted gene co-expression network analysis (WGCNA) and machine learning (ML) began to be applied to the screening of potential disease targets. WGCNA is a new bioinformatics approach that constructs a scale-free network by linking gene expression levels with clinical features to screen for modules and genes highly associated with disease [12]. ML algorithms such as least absolute shrinkage and selection operator (LASSO), support vector machine recursive feature elimination (SVM-RFE), and random forest (RF) are also widely used in bioinformatics research to screen potential targets of diseases and construct accurate diagnostic models.

This study analyzed the mRNA datasets of AMI and IHF in the GEO database and tried to find the co-expressed modules between these two diseases using WGCNA. We used enrichment analysis to identify pathways and biological functions involved in IHF after AMI. Subsequently, we screened potential biomarkers with three machine learning algorithms: SVM-REF, LASSO, and RF. We input the

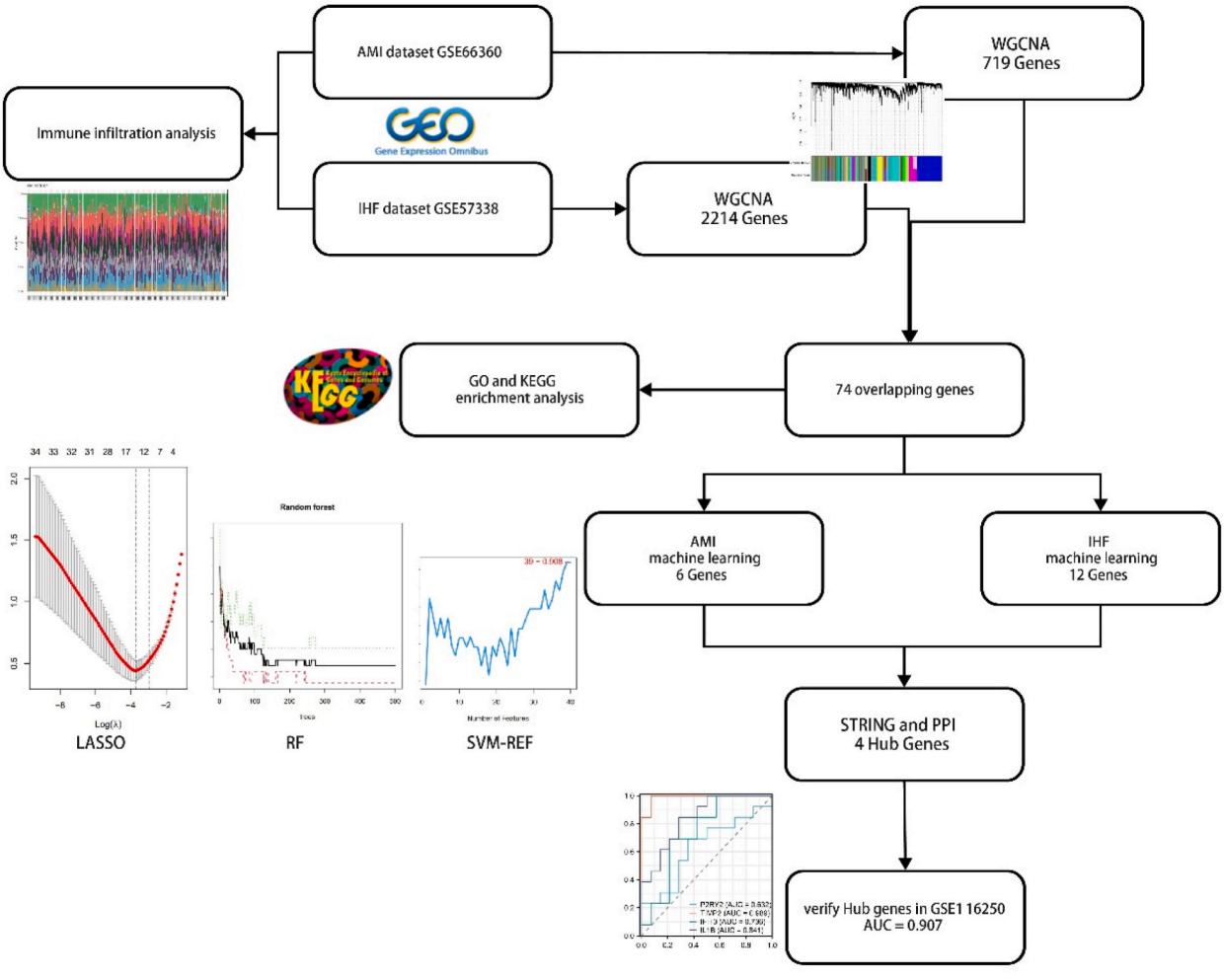

Fig. 1. The study flowchart. This is a summary of our study as a whole.

results obtained by machine learning into the STRING database to determine the relationship between proteins, thereby obtaining the Hub gene and verifying it in an external dataset. In addition, we performed immune cell infiltration analysis on the AMI and IHF datasets, helping us to understand the role of immune cells in the development of IHF after AMI. Fig. 1 depicts the study flowchart.

2. Materials and methods

2.1. Data acquisition and preprocessing

We downloaded the disease dataset from the GEO database [13]. We chose GSE66360 as the dataset for AMI (circulating endothelial cell samples from 49 patients with acute myocardial infarction and 50 controls) [14]. We chose GSE57338 as the dataset for ischemic heart failure (left ventricular myocardium samples from 95 patients with ischemic heart failure and 136 controls) [15]. We finished the preparation of the data using R program (version 4.2.0). We eliminated the probes that corresponded to several compounds and changed the probe ID into a gene symbol in accordance with the platform's annotation file. Only the probe with the highest signal value is kept when there are several probes relating to the same molecule. Lastly, we eliminate the data's batch effects. We chose GSE116250 as the validation set of results. The basic information of all data sets was shown in Table 1.

2.2. Weighted gene Co-expression network analysis

We performed WGCNA on GSE66360 and GSE57338, respectively, to obtain modules closely related to AMI and IHF. Following a filtering criterion of 0.5, the first step involved eliminating genes and samples that didn't meet the criteria using the goodSamplesGenes function. This was followed by the construction of a scale-free co-expression network. For the purpose of calculating adjacencies, a soft threshold of $\beta = 30$ and a scale-free fit of $R2 = 0.9$ were utilized. These adjacencies were subsequently converted into a topological overlap matrix (TOM), which was used for assessing gene ratios and dissimilarities. Genes with comparable expression patterns were grouped into modules through the process of average linkage hierarchical clustering. Preferring larger groupings, the threshold for module size was established at a minimum of 200. The next step involved determining the dissimilarity between the module eigengenes. This process involved selecting a cut-off point on the module dendrogram to merge several modules for additional analysis. Finally, the eigengene network was visualized. Lastly, to identify the key genes of IHF after AMI, the important modules of both AMI and IHF were intersected. Finally, we took the intersection of the important modules of AMI and IHF as the key genes of IHF after AMI.

2.3. Functional Enrichment Analysis

We conducted Gene Ontology (GO) and Kyoto Encyclopedia of Genes and Genomes (KEGG) enrichment analysis and visualization utilizing the clusterProfiler package [16–18]. This analysis was applied to key genes to investigate the biological functions and signaling pathways implicated in IHF after AMI.

2.4. Machine learning

We employed three machine learning algorithms, namely LASSO, RF, and SVM-RFE, to perform a comprehensive screening of candidate genes associated with IHF after AMI [19–21]. To implement the LASSO algorithm, we utilized the glmnet package, employing ten-fold cross-validation to identify significant genes. The RF algorithm was executed using the randomForest package, wherein we selected the top 30 genes as potential candidates. For the SVM-RFE algorithm, we leveraged the e1071 package and determined the optimal number of genes based on their accuracy. The resultant gene list comprised the key genes, and we applied the three machine learning algorithms separately to identify candidate genes for AMI and IHF. Finally, by intersecting the outcomes obtained from the three distinct machine learning approaches, we derived the candidate genes associated with both AMI and IHF.

2.5. Protein–protein interaction network construction

To comprehend the progression from AMI to IHF and to uncover the interactions among protein-coding genes, we constructed a Protein-Protein Interaction (PPI) network using the STRING database [22]. We input the candidate genes associated with AMI and IHF into the STRING database to ascertain the interconnections among these genes. The parameters set for this analysis included: Network type as a full STRING network, the significance of network edges defined by evidence, and a minimum interaction score set at medium confidence (0.400). Then, we imported the results into Cytoscape3.6.1, and established a Bayesian network starting from the candidate

Table 1
The details of datasets.

Series	Platforms	Samples	tissue	Type
GSE57338	GPL11532	95 IHF and 136 Con	heart left ventricle	mRNA
GSE66360	GPL570	49 AMI and 50 Con	CD146+Circulating Endothelial Cells	mRNA
GSE116250	GPL16791	13 IHF and 14 Con	left ventricle	mRNA

genes of AMI and ending with the candidate genes of IHF. Based on the network results, we completed Hub gene selection and subsequent analysis [23].

2.6. Hub genes verification and diagnosis model construction

We chose GSE116250 as the validation set of Hub genes (left ventricular myocardium samples from 13 patients with ischemic heart failure and 14 controls) [24]. The pROC package was employed to develop diagnostic models for individual and combined genes. The discriminative capability of Hub genes was assessed using ROC curves. The diagnostic value was quantified by calculating the area

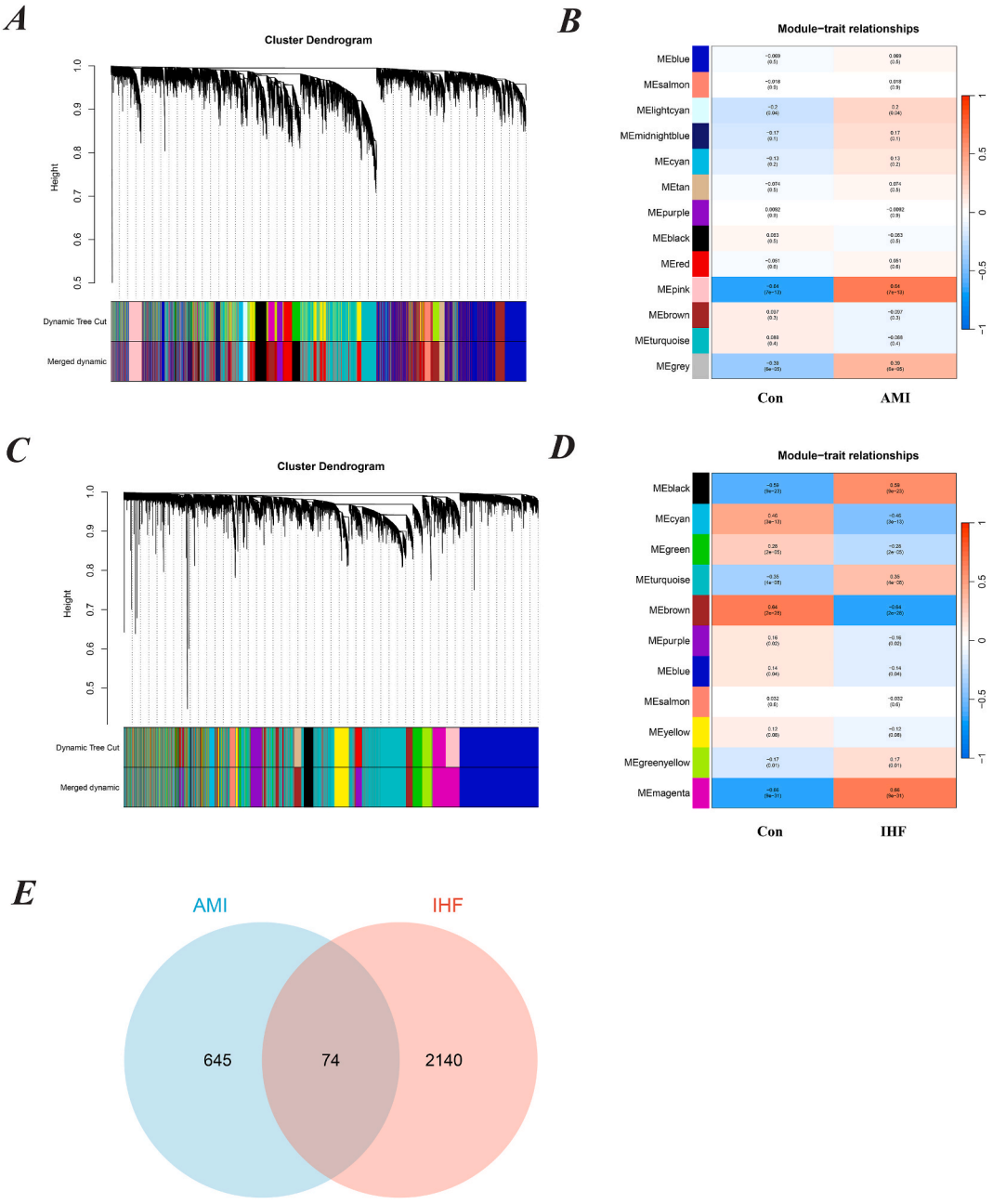

Fig. 2. WGCNA analysis result. (A) Dendrograms for gene and trait clustering in AMI were created. These gene clustering trees, or dendrograms, were derived from hierarchical clustering based on neighbor-related differences. (B) The AMI condition was characterized by 13 gene co-expression modules. Each cell within these modules displays the correlation coefficient and the corresponding p-value. (C) Dendrograms for gene and trait clustering were also constructed for IHF. (D) 11 gene co-expression modules of IHF. (E) The intersection of AMI and IHF. We intersected the results to get 74 key genes.

under the curve (AUC), with an AUC greater than 0.7 being deemed as an ideal diagnostic indicator.

2.7. Immune infiltration analysis

The CIBERSORT package was utilized to evaluate the composition of immune and stromal cells in circulating endothelial cell samples from AMI for immune cell infiltration analysis [25]. Similarly, this package was also used to assess the content of these cells in IHF myocardial samples, aiming to delineate the cellular heterogeneity in myocardial expression profiles. We plan to compare the expression of immune cells in AMI and IHF to investigate their role in the progression of heart failure post-myocardial infarction. Bar graphs will be employed to display the proportion of each immune cell type in various samples. The distribution differences in cells between the disease and normal groups will be compared using a *t*-test, setting the significance threshold at p. adj$<$0.05.

3. Results

3.1. Construction of Co-expressed gene modules

We performed WGCNA on GSE66360 and GSE57338 to obtain modules closely related to AMI and IHF, respectively. The analysis of GSE66360 shows that when the value of $\beta = 9$, the network is closer to the scale-free network. We identified 13 modules associated with AMI, among which the pink module had the highest correlation with AMI (correlation coefficient = 0.64, P = 7e-13), containing a total of 719 genes. The analysis of GSE57338 shows that when the value of $\beta = 11$, the network is closer to the scale-free network. We identified 11 modules associated with IHF, among which the black module (correlation coefficient = 0.59), brown module (correlation coefficient = 0.64), and magenta (correlation coefficient = 0.66) modules were highly correlated with IHF. Since the gene expression of the black module and the magenta module both increased in the disease group (the gene expression of the pink module of AMI also increased in the disease group), we chose the black module and the magenta module as subsequent analysis modules. The two modules contain a total of 2214 genes. We intersected the results to get 74 key genes. The relevant results are shown in Fig. 2A–E.

3.2. Functional Enrichment Analysis

GO and KEGG enrichment analyses were conducted on 74 essential genes to decipher the shared biological mechanisms underlying AMI and IHF. Categories of GO enrichment analysis include biological process (BP), cellular component (CC) and molecular function (MF). Among them, BP mainly involves myeloid leukocyte activation, positive regulation of leukocyte activation, positive regulation of cell activation, leukocyte activation involved in immune response, and leukocyte cell-cell adhesion. CC mainly involves collagen-containing extracellular matrix, specific granule, *trans*-Golgi network, Golgi apparatus subcompartment, and autophagosome. MF mainly involves receptor ligand activity, signaling receptor activator activity, cytokine activity, cytokine receptor binding, and G protein-coupled purinergic nucleotide receptor activity. KEGG enrichment analysis showed that 74 key genes were mainly enriched in

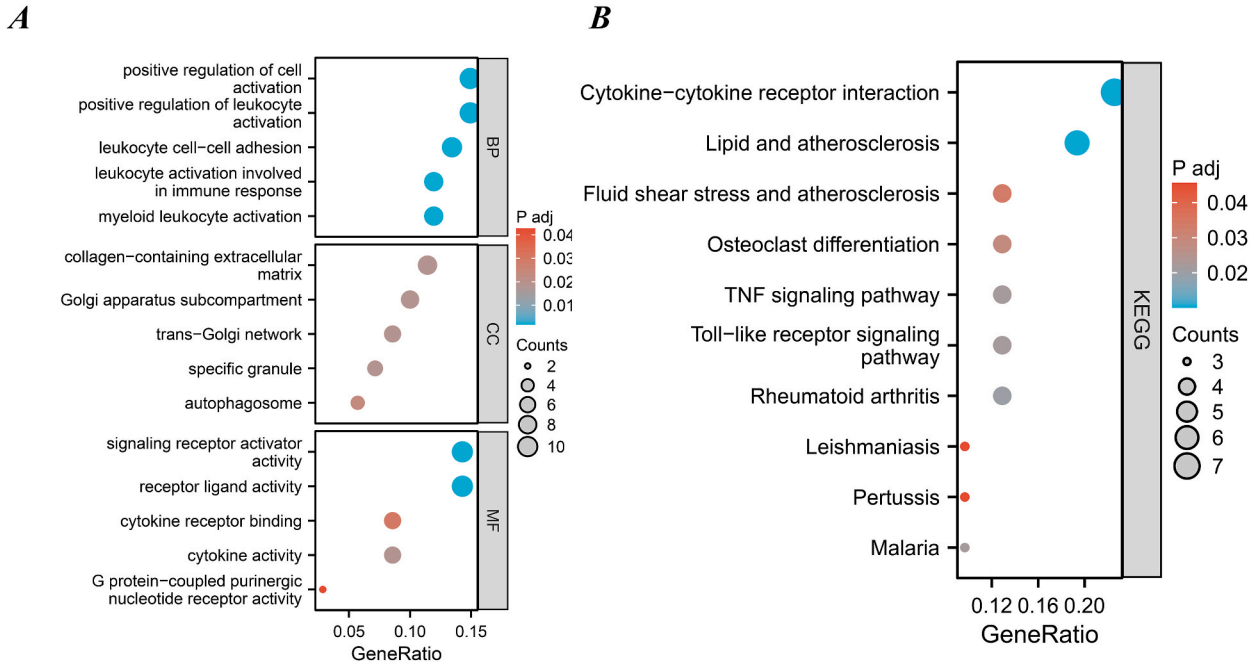

Fig. 3. Functional Enrichment Analysis of Key Genes. (A) GO enrichment analysis results. (B) KEGG enrichment analysis results.

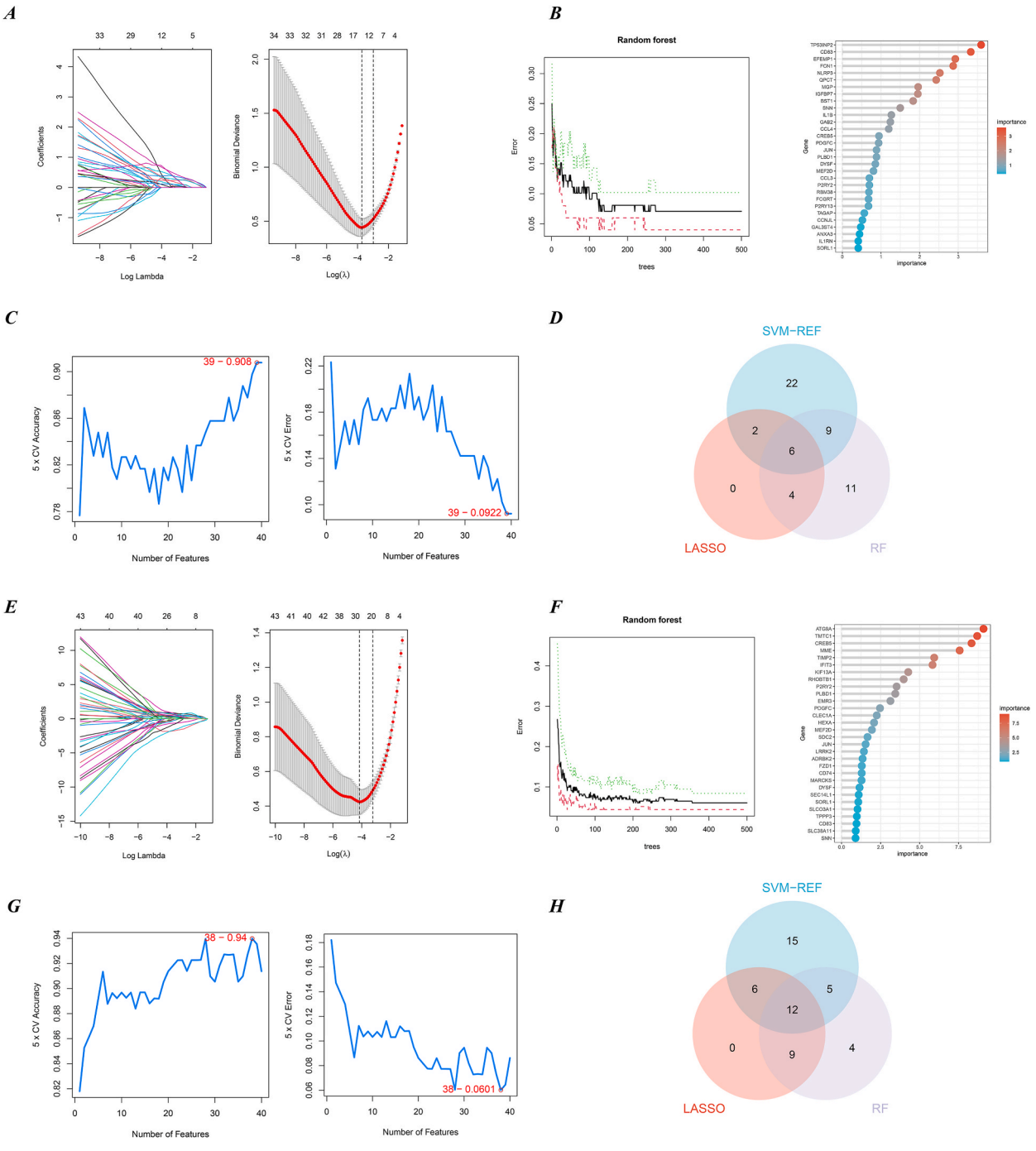

(caption on next page)

Fig. 4. Employing Machine Learning for Identifying Candidate Genes in AMI and IHF. (A) Lasso Model for AMI Gene Screening. We deployed Lasso regression to pinpoint optimal feature genes in AMI, determining the best lambda value through the minimization of partial likelihood deviance. The coefficient curves, each representing an individual gene, highlight the gene selection process. At the curve's lowest point, 12 genes (n = 12) emerged as the most suitable for the Lasso model, as indicated by the solid vertical lines depicting the partial likelihood deviance. (B) SVM-RFE Model in AMI. The SVM-RFE algorithm was utilized for an in-depth identification of feature genes, selecting those with the highest accuracy and lowest error rate as shown in the performance curves. The axes of the graph represent the number of features selected (x-axis) and the prediction accuracy (y-axis). (C) RF Model for AMI Genes. Using the Random Forest method, we calculated the relative importance of overlapping candidate genes, focusing on the top 20 genes in terms of their significance. (D) Venn Diagram for AMI Candidate Genes. A Venn diagram illustrates the intersection of the three algorithms, culminating in the identification of 6 primary candidate genes for AMI. (E) Candidate genes screening in the Lasso model of IHF. (F) Candidate genes screening in the SVM-RFE model of IHF. (G) Candidate genes screening in the RF model of IHF. (H) Venn Diagram for IHF Candidate Genes. This diagram displays the integration of results from the three applied algorithms, leading to the determination of 12 candidate genes for IHF.

Cytokine-cytokine receptor interaction, Lipid and atherosclerosis, Rheumatoid arthritis, Toll-like receptor signaling pathway, and TNF signaling pathway. We will show the top five results of GO enrichment analysis and top ten results of KEGG enrichment analysis, as shown in Fig. 3A–B. See Supplementary Table S1 for full enrichment results.

3.3. Identification of hub genes via machine learning

In this study, we employed three distinct machine learning algorithms—LASSO, Random Forest (RF), and Support Vector Machine-Recursive Feature Elimination (SVM-RFE)—to identify key hub genes associated with Acute Myocardial Infarction (AMI) and Ischemic Heart Failure (IHF). For AMI, the LASSO algorithm pinpointed 12 potential hub genes. The RF algorithm, which ranks genes based on their importance scores, yielded 30 top candidate genes. Similarly, the SVM-RFE algorithm indicated optimum accuracy with a set of 39 genes, leading us to select these as candidates. Upon intersecting the results from all three algorithms, we identified six prime candidates for AMI. In the case of IHF, the LASSO algorithm revealed 27 candidate genes. Adhering to the methodology used for AMI, the top 30 genes as per the RF algorithm were chosen. The SVM-RFE algorithm presented the highest accuracy with 38 genes, which were subsequently selected. The intersection of results from these algorithms yielded 12 leading candidate genes for IHF. Fig. 4A–H graphically represents these findings, elucidating the intersection and unique selections from each algorithm. All results of machine learning are presented in Supplementary Table S2.

3.4. PPI network construction

We input 6 AMI candidate genes and 12 IHF candidate genes into the STRING database to obtain the functional relationship between protein-coding genes. Ultimately, we identified 6 nodes and 5 interactions. Among them, IL1B of AMI and TIMP2, IFIT3, P2RY2 of IHF have an interaction relationship. Therefore, we selected four genes, IL1B, TIMP2, IFIT3, and P2RY2, as Hub genes. The visualization results are shown in Fig. 5.

3.5. Hub genes verification and diagnosis model construction

We completed the validation of the Hub gene at GSE116250. We established ROC curve analysis to verify the diagnostic value of Hub gene. In the single gene diagnostic model, TIMP2 had the highest diagnostic value (AUC = 0.989). The combined gene diagnosis model has a high diagnostic value (AUC = 0.907). The result is shown in Fig. 6A–B. The results showed that Hub gene may be an effective index for detecting IHF after AMI.

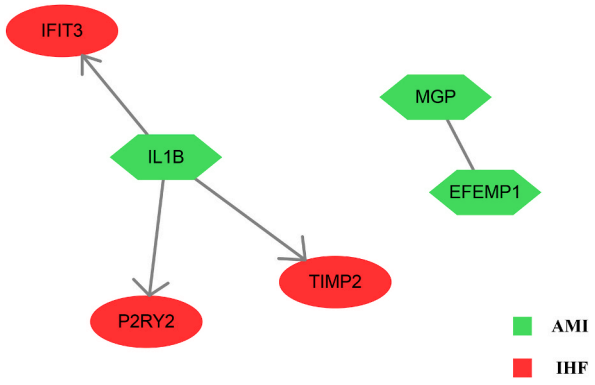

Fig. 5. A PPI network starting from the candidate genes of AMI and ending with the candidate genes of IHF.

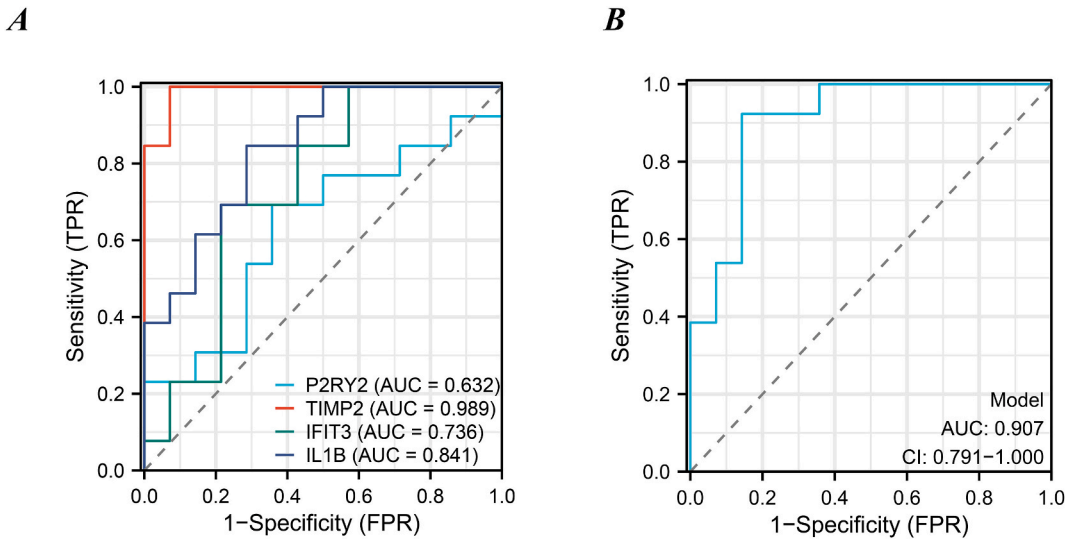

Fig. 6. Results of Diagnostic Value Assessment. (A) The ROC curve of each candidate genes in GSE116250. (B) The ROC curve of the 4-gene diagnostic model in GSE116250.

3.6. *Immune cell infiltration analysis*

To investigate the involvement of immune cells in the progression of IHF after AMI, we conducted an analysis of immune cell infiltration within both the AMI and IHF datasets using the CIBERSORT algorithm. The results of this analysis are depicted in Fig. 7A for the AMI dataset and Fig. 7C for the IHF dataset. These bar graphs distinctly illustrate the variation in immune cell subpopulation composition across the samples. In the AMI dataset specifically, we examined the diversity in immune cell makeup between the AMI

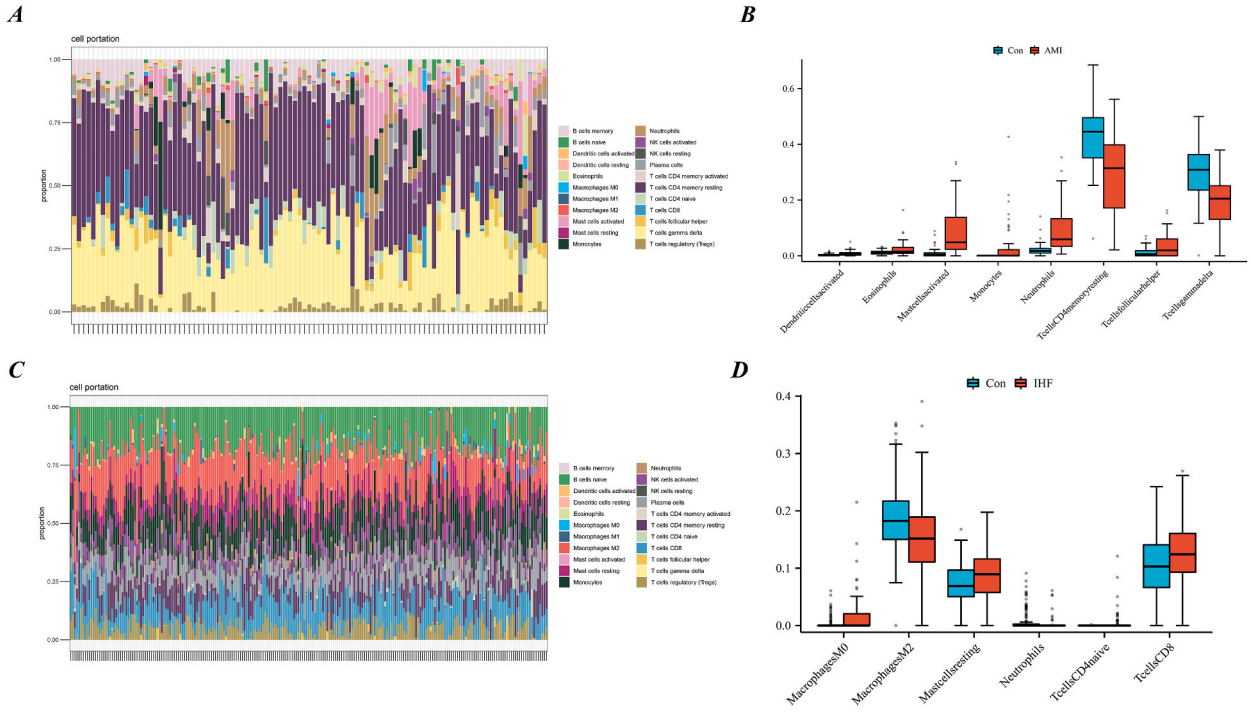

Fig. 7. Immune cell infiltration analysis. (A) This bar plot illustrates the distribution of 22 distinct immune cell types across various AMI samples, providing a comparative visual representation of their proportions. (B) The box plot depicts the expression profiles of eight immune cell types that showed significant dysregulation in AMI samples compared to control samples. (C) Similar to AMI, the bar plot for IHF samples delineates the proportion of 22 immune cell types, offering a visual comparison of their distribution in different IHF samples. (D) The box plot depicts the expression profiles of six immune cell types that showed significant dysregulation in IHF samples compared to control samples.

and control (healthy) samples. This comparison revealed significant disparities in the infiltration levels of eight distinct immune cell types, highlighting the heterogeneity of immune response in the context of AMI. Among them, Dendritic cells activated, Eosinophils, Mast cells activated, Monocytes, Neutrophils, and T cells focal helper were highly expressed in AMI samples. The expressions of T cells CD4 memory resting and T cells gamma delta were higher in the control group. The expression levels of each immune cell are shown in Fig. 7-B. In the IHF dataset, we assessed the heterogeneity of immune cell composition between IHF samples and healthy samples. The results showed that there were 6 types of immune cell infiltration with significant differences. Among them, Macrophages M0, Mast cells resting, T cells CD4 naive, and T cells CD8 were highly expressed in IHF samples. Neutrophils and Macrophages M2 were more highly expressed in the control group. The expression levels of each immune cell are shown in Fig. 7-D.

4. Discussion

AMI is one of the main causes of heart failure in patients. Finding the mechanism of IHF after AMI has important clinical significance for the prevention and treatment of heart failure. Transcript profiling is a promising tool in the search for molecular mechanisms and biomarkers. Unfortunately, for patients with AMI, although cardiac biopsy can truly reflect the pathological changes of the damaged myocardium after AMI, cardiac biopsy is often not clinically applicable. We chose peripheral blood cells for replacement, but they are still different from heart tissue. For IHF patients, transcriptomic analysis of cardiac tissue can more accurately describe the physiopathological changes of IHF. However, the lack of analysis of IHF peripheral blood samples provides certain difficulties for the development of IHF diagnostic markers. Although GSE59867 collected peripheral blood samples from 111 patients with ST-segment elevation myocardial infarction in 4 time periods, only 17 patients had detailed disease information (whether the patient developed heart failure within 6 months) in this dataset [26]. Therefore, the number of effective samples limits the application of this data set (it is generally believed that the sample size should be 4 times the number of Hub genes and at least more than 20). We had to select circulating endothelial cell samples from AMI and cardiac tissue samples from IHF for analysis.

In this study, we first identified the gene modules co-expressed by AMI and IHF through WGCNA, and a total of 74 genes were obtained. Subsequently, we explored the common biological functions and signaling pathways involved in AMI and IHF through GO and KEGG enrichment analysis. The results showed that the common mechanisms of AMI and IHF are mostly related to inflammation and immunity, which may be the key mechanisms connecting these two diseases. AMI can lead to myocardial necrosis in the infarcted area, and inflammatory cells such as monocytes and macrophages migrate to the damaged area to remove dead cells after AMI, and participate in subsequent damage and repair [27]. Leukocytes are recruited to the damaged myocardium, but the myocardium away from the infarct is also inflamed, which may be responsible for the remodeling of the non-infarcted myocardium [28]. At the same time, a large number of cytokines such as TNF-α, IL-6, IL-10, and IL1 are released into the blood, which participate in physiological processes such as inflammatory response and angiogenesis, and affect the remodeling of the heart and the establishment of collateral circulation [29,30]. Toll-like receptor (TLR) signaling pathway and TNF signaling pathway in the KEGG enrichment results also connect AMI and IHF. TLR signaling pathway is involved in the inflammatory response. Studies have shown that AMI is accompanied by increased expression of TLR2 and TLR4 on circulating monocytes [31]. In animal models, blocking TLR2/4 signaling reduced inflammatory cell influx and infarct size. Inhibition of TLR4 can reduce AMI-induced cardiomyocyte oxidative stress and apoptosis [32]. In a mouse model, TLR2, while involved in cardiac remodeling after AMI, also promoted the inflammatory response of heart failure myocardium [33]. Cardiomyocyte apoptosis induced by TLR4 also aggravates the degree of IHF [34]. TNF ligands can induce multiple effects in the myocardium, including apoptosis, hypertrophy, inflammation, and extracellular matrix remodeling [35]. Therefore, inflammatory factors and chemokines such as TNF-α, IL-6, IL-1, etc. are designed as new therapeutic targets for AMI and IHF [36]. In short, through enrichment analysis and previous studies, we believe that inflammatory factor secretion and immune cell recruitment are common mechanisms of AMI and IHF.

Subsequently, we screened the co-expressed genes with 3 machine learning algorithms, and obtained 6 candidate genes for AMI and 12 candidate genes for IHF. We obtained the protein interaction relationship through the STRING database, and finally identified four Hub genes, IL1B, TIMP2, IFIT3, and P2RY2. The verification results in external data sets also showed that these four Hub genes have high diagnostic value.

Interleukin-1 Beta (IL1B) is a cytokine produced by activated macrophages that is involved in a variety of cellular activities, including cell proliferation, differentiation, and apoptosis. Pro-inflammatory functions are activated upon binding of IL1B to its receptors, IL-1R1 and IL-1R3 [37]. Thus, IL1B plays an important role in the sterile inflammatory response and subsequent adverse cardiac remodeling after AMI [38]. Studies have shown that the expression of IL1B after AMI is mainly concentrated in the myocardium, spleen, and peripheral blood, especially in the myocardium [39]. The results of this study also make up for the deficiency that we selected circulating endothelial cells for AMI samples (lack of IL1B expression results in AMI cardiomyocyte samples). In the serum of patients with heart failure, IL1B levels are highly abnormal and remain elevated after mechanical circulatory support. This indicates that IL1B elevation may run through the entire process of the development of IHF after AMI [40]. Targeting IL1B therapy has also achieved good results in animal experiments. Studies have shown that after 10 weeks of monoclonal antibody treatment of IL1B in mice with IHF after AMI, it can prevent the further deterioration of left ventricular systolic function and diastolic function of the mouse heart, and restore the contractile reserve [41]. Although targeting IL1B did not affect inflammasome formation or caspase-1 activation after AMI, it did reduce cardiomyocyte apoptosis and limit LV enlargement after AMI [42]. It is worth noting that although cytokine therapy targeting IL1B appears promising in animals, clinical trials are still needed to further prove its efficacy [43].

Tissue inhibitor of metalloproteinases 2 (TIMP2) is a natural inhibitor of matrix metalloproteinases (MMPs), inhibiting MMP-induced extracellular matrix remodeling [44]. Studies have shown that circulating levels of MMP-2 are closely related to infarct size and left ventricular dysfunction in STEMI patients, and its expression has a complex time-dependence [45,46]. Therefore, MMP

can be used as an early measurement index of infarct size and ventricular dysfunction after infarction. Because of this, the compensatory secretion of TIMP2 after AMI also makes it valuable for detection. Studies have shown that both MMP2 and TIMP2 are highly expressed in coronary artery thrombus [47]. In conclusion, MMPs increase after myocardial infarction, leading to degradation of extracellular matrix in the infarct area and LV remodeling [48]. The MMP inhibitory function of TIMP2 is a key factor in cardiac remodeling after AMI. Therefore, TIMP2 not only has potential therapeutic value, but also has predictive value for cardiac dysfunction after infarction [49].

Interferon induced protein with tetratricopeptide repeats 3 (IFIT3) is a type I interferon-induced antiviral protein but is also involved in nonviral pathology [50]. In the previous bioinformatics studies, although the analysis methods and analysis angles were different, it was concluded that IFIT3 was the key gene of ischemic cardiomyopathy [51–53]. In vitro experiments also proved that knocking down IFIT3 can effectively inhibit the release of inflammatory cytokines and alleviate ischemia-reperfusion injury [54]. In a mouse model of coronary artery ligation, silencing of IFIT3 significantly improved cardiac function and reduced infarct size, myocardial fibrosis, and collagen content [55]. Therefore, IFIT3 may be a potential therapeutic target for AMI and IHF.

Purinergic Receptor P2Y2 (P2RY2), belonging to the P2 receptor family, is activated by extracellular nucleotides and participates in various cellular functions such as proliferation, apoptosis, and inflammation. Early infarction, activation of P2RY2 leads to persistent, nonspecific cation currents. This depolarizing current induces cellular automaticity, triggering arrhythmic events [56]. Ischemia-reperfusion injury will compensatory increase the expression of P2RY2 to resist apoptosis. The mechanism may be related to inhibition of YAP phosphorylation and reduction of mitochondrial fission [57]. In addition, the mRNA level of P2RY2 was increased 4.7-fold in the left ventricular myocardium of rats with congestive heart failure [58]. Therefore, P2RY2 has potential as a therapeutic target for AMI and IHF and deserves further study.

After an AMI occurs, Neutrophils are among the first cells to reach the infarct area, where they accumulate within the first few hours, triggering inflammation and tissue destruction [59]. The proteases and bioactive substances contained in Neutrophils include MMPs, neutrophil extracellular traps (NETs), and NADPH oxidase, etc. NETs will cross-link with plasma fibrinogen, leading to thrombosis and coronary no-reflow phenomenon, and aggravating myocardial infarction [60]. Eosinophils and Monocytes peaked on the third day after AMI [61,62]. Eosinophils mainly increase myocardial tissue damage by generating ROS through peroxidase. However, IL-4 secreted by it can also inhibit cardiomyocyte apoptosis, prevent neutrophils from adhering to the endothelial wall, and improve cardiac dysfunction [63]. Monocytes are not only involved in the breakdown of necrotic myocardium, but also one of the reasons for the further recruitment of neutrophils [64]. Mast cells originate from the bone marrow and can produce a variety of inflammatory cytokines, including IFNG, IL-6, and TNF-α, which participate in the inflammation and fibrosis process of myocardial infarction and heart failure [65]. The results of immunoassays showed that the status of Mast cells in AMI and IHF is different, which may be because Mast cells are mainly involved in the regulation of fibrous tissue metabolism in the process of myocardial remodeling, but there is still a lack of research in this area [66]. There was no similarity between AMI and IHF in terms of immune cell infiltration, which may be explained by differences in myocardial samples and circulating endothelial cell samples. Even so, mounting evidence for the contribution of immune-modifying therapies to cardiac repair and myocardial fibrosis has become an exciting area of research [67].

The novelty of our study is as follows. First, we identified the co-expressed genes of AMI and IHF by WGCNA. Secondly, we identified 4 Hub genes through 3 machine learning algorithms and the PPI network constructed by STRING, and verified them in external datasets, which provided new ideas for our understanding of the molecular mechanism of IHF development after AMI. In addition, our enrichment analysis and immune infiltration analysis of AMI and IHF showed that the molecular mechanisms of the two are closely related to inflammation and immunity, which provides ideas for us to develop new treatments to reduce the development of IHF after AMI.

Nevertheless, there are still some shortcomings in this study. Differences in sample sources may lead to bias in the results, but there is indeed a lack of data sets with sufficient sample sizes. Second, it is unclear whether increased mRNA levels lead to a parallel increase in protein expression, and the execution of many biological functions also relies on post-translational modifications. In future studies, if conditions permit, we will increase the experimental design to evaluate protein levels to further verify our conclusions.

5. Conclusion

We performed bioinformatics analysis on the GEO dataset to explore the underlying molecular mechanisms, key genes, and immune cell infiltration environment for the development of IHF after AMI. Through three machine learning algorithms, LASSO, RF, and SVM-RFE, we identified four genes, IL1B, TIMP2, IFIT3, and P2RY2, as potential therapeutic targets and biomarkers for the development of IHF after AMI. More importantly, based on the diagnostic model of these 4 genes, we have generated a new understanding of the pathogenesis of IHF after AMI and may be an interesting target for future in-depth studies.

Consent for publication

Not applicable.

Ethics approval and consent to participate

Not applicable.

Funding

Our work was supported by the National Natural Science Foundation of China [Grants nos. 81774247; 81804045] and Shandong TCM Science and Technology Project [Grants nos. 2021Q114].

Data availability statement

Publicly available datasets were analyzed in this study. This data can be found here: GSE66360; GSE57338; GSE116250.

CRediT authorship contribution statement

Yan Li: Writing – original draft, Methodology, Conceptualization. **Ying Hu:** Writing – review & editing, Visualization. **Feng Jiang:** Writing – review & editing, Visualization. **Haoyu Chen:** Writing – review & editing, Visualization. **Yitao Xue:** Writing – review & editing, Supervision, Formal analysis. **Yiding Yu:** Writing – review & editing, Supervision, Formal analysis, Conceptualization.

Declaration of competing interest

The authors declare that they have no known competing financial interests or personal relationships that could have appeared to influence the work reported in this paper.

Acknowledgements

Not applicable.

Appendix A. Supplementary data

Supplementary data to this article can be found online at https://doi.org/10.1016/j.heliyon.2024.e27165.

References

[1] A.P. DeFilippis, A.R. Chapman, N.L. Mills, et al., Assessment and treatment of patients with type 2 myocardial infarction and acute nonischemic myocardial injury, Circulation 140 (20) (2019) 1661–1678, https://doi.org/10.1161/CIRCULATIONAHA.119.040631.
[2] P.A. Heidenreich, B. Bozkurt, D. Aguilar, et al., 2022 AHA/ACC/HFSA guideline for the management of heart failure: a report of the American college of cardiology/American heart association joint committee on clinical practice guidelines, J. Am. Coll. Cardiol. 79 (17) (2022) e263–e421.
[3] E.J. Benjamin, M.J. Blaha, S.E. Chiuve, et al., Heart disease and stroke statistics—2017 update: a report from the American Heart Association, Circulation 135 (10) (2017) e146–e603.
[4] M.C. Bahit, A. Kochar, C.B. Granger, Post-myocardial infarction heart failure, JACC (J. Am. Coll. Cardiol.): Heart Fail. 6 (3) (2018) 179–186.
[5] J.J. McMurray, S. Adamopoulos, S.D. Anker, et al., ESC guidelines for the diagnosis and treatment of acute and chronic heart failure 2012: the task force for the diagnosis and treatment of acute and chronic heart failure 2012 of the European society of cardiology. Developed in collaboration with the heart failure association (HFA) of the ESC [published correction appears in eur heart J. 2013 Jan;34(2):158], Eur. Heart J. 33 (14) (2012) 1787–1847, https://doi.org/10.1093/eurheartj/ehs104.
[6] M. Radovanovic, Z. Vasiljevic, N. Radovanovic, et al., B-type natriuretic peptide in outpatients after myocardial infarction: optimized cut-off value for incident heart failure prediction, Peptides 31 (10) (2010) 1946–1948, https://doi.org/10.1016/j.peptides.2010.06.023.
[7] A. Driscoll, E.H. Barnes, S. Blankenberg, et al., Predictors of incident heart failure in patients after an acute coronary syndrome: the LIPID heart failure risk-prediction model, Int. J. Cardiol. 248 (2017) 361–368, https://doi.org/10.1016/j.ijcard.2017.06.098.
[8] K.T. Moe, P. Wong, Current trends in diagnostic biomarkers of acute coronary syndrome, Ann. Acad. Med. Singapore 39 (3) (2010) 210–215.
[9] X. Li, B. Li, H. Jiang, Identification of time-series differentially expressed genes and pathways associated with heart failure post-myocardial infarction using integrated bioinformatics analysis, Mol. Med. Rep. 19 (6) (2019) 5281–5290, https://doi.org/10.3892/mmr.2019.10190.
[10] J. Zhang, J. Wang, Y. Wu, W. Li, K. Gong, P. Zhao, Identification of SLED1 as a potential predictive biomarker and therapeutic target of post-infarct heart failure by bioinformatics analyses, Int. Heart J. 62 (1) (2021) 23–32, https://doi.org/10.1536/ihj.20-439.
[11] X. Kong, H. Sun, K. Wei, et al., WGCNA combined with machine learning algorithms for analyzing key genes and immune cell infiltration in heart failure due to ischemic cardiomyopathy, Front Cardiovasc Med 10 (2023) 1058834, https://doi.org/10.3389/fcvm.2023.1058834. Published 2023 Mar 17.
[12] P. Langfelder, S. Horvath, WGCNA: an R package for weighted correlation network analysis, BMC Bioinf. 9 (2008) 559, https://doi.org/10.1186/1471-2105-9-559. Published 2008 Dec 29.
[13] T. Barrett, S.E. Wilhite, P. Ledoux, et al., NCBI GEO: archive for functional genomics data sets–update, Nucleic Acids Res. 41 (Database issue) (2013) D991–D995, https://doi.org/10.1093/nar/gks1193.
[14] E.D. Muse, E.R. Kramer, H. Wang, et al., A whole blood molecular signature for acute myocardial infarction, Sci. Rep. 7 (1) (2017) 12268, https://doi.org/10.1038/s41598-017-12166-0. Published 2017 Sep. 25.
[15] Y. Liu, M. Morley, J. Brandimarto, et al., RNA-Seq identifies novel myocardial gene expression signatures of heart failure, Genomics 105 (2) (2015) 83–89, https://doi.org/10.1016/j.ygeno.2014.12.002.
[16] G. Yu, L.G. Wang, Y. Han, Q.Y. He, clusterProfiler: an R package for comparing biological themes among gene clusters, OMICS 16 (5) (2012) 284–287, https://doi.org/10.1089/omi.2011.0118.
[17] The Gene Ontology Consortium, The gene Ontology resource: 20 years and still GOing strong, Nucleic Acids Res. 47 (D1) (2019) D330–D338, https://doi.org/10.1093/nar/gky1055.
[18] M. Kanehisa, S. Goto, KEGG: kyoto encyclopedia of genes and genomes, Nucleic Acids Res. 28 (1) (2000) 27–30, https://doi.org/10.1093/nar/28.1.27.
[19] J. Friedman, T. Hastie, R. Tibshirani, Regularization paths for generalized linear models via coordinate descent, J. Stat. Software 33 (1) (2010) 1–22.

[20] F. Petralia, P. Wang, J. Yang, Z. Tu, Integrative random forest for gene regulatory network inference, Bioinformatics 31 (12) (2015) i197–i205, https://doi.org/10.1093/bioinformatics/btv268.

[21] S. Huang, N. Cai, P.P. Pacheco, S. Narrandes, Y. Wang, W. Xu, Applications of support vector machine (SVM) learning in cancer genomics, Cancer Genomics Proteomics 15 (1) (2018) 41–51, https://doi.org/10.21873/cgp.20063.

[22] D. Szklarczyk, A.L. Gable, K.C. Nastou, et al., The STRING database in 2021: customizable protein-protein networks, and functional characterization of user-uploaded gene/measurement sets [published correction appears in Nucleic Acids Res. 2021 Oct 11;49(18):10800], Nucleic Acids Res. 49 (D1) (2021) D605–D612, https://doi.org/10.1093/nar/gkaa1074.

[23] P. Shannon, A. Markiel, O. Ozier, et al., Cytoscape: a software environment for integrated models of biomolecular interaction networks, Genome Res. 13 (11) (2003) 2498–2504, https://doi.org/10.1101/gr.1239303.

[24] T. Yamaguchi, T.S. Sumida, S. Nomura, et al., Cardiac dopamine D1 receptor triggers ventricular arrhythmia in chronic heart failure, Nat. Commun. 11 (1) (2020) 4364, https://doi.org/10.1038/s41467-020-18128-x. Published 2020 Aug 31.

[25] A.M. Newman, C.L. Liu, M.R. Green, et al., Robust enumeration of cell subsets from tissue expression profiles, Nat. Methods 12 (5) (2015) 453–457, https://doi.org/10.1038/nmeth.3337.

[26] A. Maciejak, M. Kiliszek, M. Michalak, et al., Gene expression profiling reveals potential prognostic biomarkers associated with the progression of heart failure, Genome Med. 7 (1) (2015) 26, https://doi.org/10.1186/s13073-015-0149-z. Published 2015 Mar 14.

[27] Y. Jian, X. Zhou, W. Shan, et al., Crosstalk between macrophages and cardiac cells after myocardial infarction, Cell Commun. Signal. 21 (1) (2023) 109, https://doi.org/10.1186/s12964-023-01105-4. Published 2023 May 11.

[28] N. Ruparelia, J.E. Digby, A. Jefferson, et al., Myocardial infarction causes inflammation and leukocyte recruitment at remote sites in the myocardium and in the renal glomerulus, Inflamm. Res. 62 (5) (2013) 515–525, https://doi.org/10.1007/s00011-013-0605-4.

[29] A. Mitsis, N.P.E. Kadoglou, V. Lambadiari, et al., Prognostic role of inflammatory cytokines and novel adipokines in acute myocardial infarction: an updated and comprehensive review, Cytokine 153 (2022) 155848, https://doi.org/10.1016/j.cyto.2022.155848.

[30] W. He, P. Chen, Q. Chen, Z. Cai, P. Zhang, Cytokine storm: behind the scenes of the collateral circulation after acute myocardial infarction, Inflamm. Res. 71 (10–11) (2022) 1143–1158, https://doi.org/10.1007/s00011-022-01611-0.

[31] T.C. van der Pouw Kraan, F.J. Bernink, C. Yildirim, et al., Systemic toll-like receptor and interleukin-18 pathway activation in patients with acute ST elevation myocardial infarction, J. Mol. Cell. Cardiol. 67 (2014) 94–102, https://doi.org/10.1016/j.yjmcc.2013.12.021.

[32] H. Li, H. Yang, D. Wang, L. Zhang, T. Ma, Peroxiredoxin2 (Prdx2) reduces oxidative stress and apoptosis of myocardial cells induced by acute myocardial infarction by inhibiting the TLR4/nuclear factor kappa B (NF-κB) signaling pathway, Med. Sci. Mon. Int. Med. J. Exp. Clin. Res. 26 (3) (2020) e926281, https://doi.org/10.12659/MSM.926281. Published 2020 Dec.

[33] T. Shishido, N. Nozaki, S. Yamaguchi, et al., Toll-like receptor-2 modulates ventricular remodeling after myocardial infarction, Circulation 108 (23) (2003) 2905–2910, https://doi.org/10.1161/01.CIR.0000101921.93016.1C.

[34] Z.W. Liu, H.T. Zhu, K.L. Chen, C. Qiu, K.F. Tang, X.L. Niu, Selenium attenuates high glucose-induced ROS/TLR-4 involved apoptosis of rat cardiomyocyte, Biol. Trace Elem. Res. 156 (1–3) (2013) 262–270, https://doi.org/10.1007/s12011-013-9857-7.

[35] T. Ueland, A. Yndestad, C.P. Dahl, L. Gullestad, P. Aukrust, TNF revisited: osteoprotegerin and TNF-related molecules in heart failure, Curr. Heart Fail. Rep. 9 (2) (2012) 92–100, https://doi.org/10.1007/s11897-012-0088-6.

[36] A. Hanna, N.G. Frangogiannis, Inflammatory cytokines and chemokines as therapeutic targets in heart failure, Cardiovasc. Drugs Ther. 34 (6) (2020) 849–863, https://doi.org/10.1007/s10557-020-07071-0.

[37] A. Abbate, S. Toldo, C. Marchetti, J. Kron, B.W. Van Tassell, C.A. Dinarello, Interleukin-1 and the inflammasome as therapeutic targets in cardiovascular disease, Circ. Res. 126 (9) (2020) 1260–1280, https://doi.org/10.1161/CIRCRESAHA.120.315937.

[38] Z. Li, S. Hu, K. Huang, T. Su, J. Cores, K. Cheng, Targeted anti-IL-1β platelet microparticles for cardiac detoxing and repair, Sci. Adv. 6 (6) (2020) eaay0589, https://doi.org/10.1126/sciadv.aay0589. Published 2020 Feb 5.

[39] F. Mo, Y. Luo, Y. Yan, J. Li, S. Lai, W. Wu, Are activated B cells involved in the process of myocardial fibrosis after acute myocardial infarction? An in vivo experiment, BMC Cardiovasc. Disord. 21 (1) (2021), https://doi.org/10.1186/s12872-020-01775-9, 5. Published 2021 Jan 6.

[40] N. Niazy, L. Mrozek, M. Barth, et al., Altered mRNA expression of interleukin-1 receptors in myocardial tissue of patients with left ventricular assist device support, J. Clin. Med. 10 (21) (2021) 4856, https://doi.org/10.3390/jcm10214856. Published 2021 Oct 22.

[41] S. Toldo, E. Mezzaroma, E. Bressi, et al., Interleukin-1β blockade improves left ventricular systolic/diastolic function and restores contractility reserve in severe ischemic cardiomyopathy in the mouse, J. Cardiovasc. Pharmacol. 64 (1) (2014) 1–6, https://doi.org/10.1097/FJC.0000000000000106.

[42] S. Toldo, E. Mezzaroma, B.W. Van Tassell, et al., Interleukin-1β blockade improves cardiac remodelling after myocardial infarction without interrupting the inflammasome in the mouse, Exp. Physiol. 98 (3) (2013) 734–745, https://doi.org/10.1113/expphysiol.2012.069831.

[43] F.S. Heydari, S. Zare, A. Roohbakhsh, Inhibition of interleukin-1 in the treatment of selected cardiovascular complications, Curr Rev Clin Exp Pharmacol 16 (3) (2021) 219–227, https://doi.org/10.2174/1574884715666200716145935.

[44] G. Kremastiotis, I. Handa, C. Jackson, S. George, J. Johnson, Disparate effects of MMP and TIMP modulation on coronary atherosclerosis and associated myocardial fibrosis, Sci. Rep. 11 (1) (2021) 23081, https://doi.org/10.1038/s41598-021-02508-4. Published 2021 Nov 30.

[45] L. Nilsson, J. Hallén, D. Atar, L. Jonasson, E. Swahn, Early measurements of plasma matrix metalloproteinase-2 predict infarct size and ventricular dysfunction in ST-elevation myocardial infarction, Heart 98 (1) (2012) 31–36, https://doi.org/10.1136/heartjnl-2011-300079.

[46] X. Li, O.J. de Boer, H. Ploegmaker, et al., Granulocytes in coronary thrombus evolution after myocardial infarction–time-dependent changes in expression of matrix metalloproteinases, Cardiovasc. Pathol. 25 (1) (2016) 40–46, https://doi.org/10.1016/j.carpath.2015.09.007.

[47] J. Nordeng, H. Schandiz, S. Solheim, et al., TIMP-1 expression in coronary thrombi associate with myocardial injury in ST-elevation myocardial infarction patients, Coron. Artery Dis. 33 (6) (2022) 446–455, https://doi.org/10.1097/MCA.0000000000001128.

[48] K.Y. DeLeon-Pennell, C.A. Meschiari, M. Jung, M.L. Lindsey, Matrix metalloproteinases in myocardial infarction and heart failure, Prog Mol Biol Transl Sci 147 (2017) 75–100, https://doi.org/10.1016/bs.pmbts.2017.02.001.

[49] V. Kandalam, R. Basu, T. Abraham, et al., TIMP2 deficiency accelerates adverse post-myocardial infarction remodeling because of enhanced MT1-MMP activity despite lack of MMP2 activation, Circ. Res. 106 (4) (2010) 796–808, https://doi.org/10.1161/CIRCRESAHA.109.209189.

[50] J.H. Franco, S. Chattopadhyay, Z.K. Pan, How different pathologies are affected by IFIT expression, Viruses 15 (2) (2023) 342, https://doi.org/10.3390/v15020342. Published 2023 Jan 25.

[51] H. Yu, M. Yu, Z. Li, E. Zhang, H. Ma, Identification and analysis of mitochondria-related key genes of heart failure, J. Transl. Med. 20 (1) (2022) 410, https://doi.org/10.1186/s12967-022-03605-2. Published 2022 Sep. 7.

[52] C. Chen, J. Tian, Z. He, W. Xiong, Y. He, S. Liu, Identified three interferon induced proteins as novel biomarkers of human ischemic cardiomyopathy, Int. J. Mol. Sci. 22 (23) (2021) 13116, https://doi.org/10.3390/ijms222313116. Published 2021 Dec 4.

[53] Y. Yang, W. Yang, W. Huo, P. Huo, H. Yang, Identification of biomarkers for ischemic cardiomyopathy based on microarray data analysis, Cardiol. J. 24 (3) (2017) 305–313, https://doi.org/10.5603/CJ.a2017.0005.

[54] G. Guan, Y. Shen, Q. Yu, et al., Down-regulation of IFIT3 protects liver from ischemia-reperfusion injury, Int. Immunopharm. 60 (2018) 170–178, https://doi.org/10.1016/j.intimp.2018.04.045.

[55] J. Sun, Q. Zhang, X. Liu, X. Shang, Downregulation of interferon-induced protein with tetratricopeptide repeats 3 relieves the inflammatory response and myocardial fibrosis of mice with myocardial infarction and improves their cardiac function, Exp. Anim. 70 (4) (2021) 522–531, https://doi.org/10.1538/expanim.21-0060.

[56] J. Alvarez, A. Coulombe, O. Cazorla, et al., ATP/UTP activate cation-permeable channels with TRPC3/7 properties in rat cardiomyocytes, Am. J. Physiol. Heart Circ. Physiol. 295 (1) (2008) H21–H28, https://doi.org/10.1152/ajpheart.00135.2008.

[57] L.X. Xue, S.F. Chen, S.X. Xue, X.Z. Zhang, Y.J. Lian, P2RY2 alleviates cerebral ischemia-reperfusion injury by inhibiting YAP phosphorylation and reducing mitochondrial fission, Neuroscience 480 (2022) 155–166, https://doi.org/10.1016/j.neuroscience.2021.11.013.

[58] M. Hou, M. Malmsjö, S. Möller, et al., Increase in cardiac P2X1-and P2Y2-receptor mRNA levels in congestive heart failure, Life Sci. 65 (11) (1999) 1195–1206, https://doi.org/10.1016/s0024-3205(99)00353-7.
[59] Y. Ma, A. Yabluchanskiy, M.L. Lindsey, Neutrophil roles in left ventricular remodeling following myocardial infarction, Fibrogenesis Tissue Repair 6 (1) (2013) 11, https://doi.org/10.1186/1755-1536-6-11. Published 2013 Jun 3.
[60] L. Ge, X. Zhou, W.J. Ji, et al., Neutrophil extracellular traps in ischemia-reperfusion injury-induced myocardial no-reflow: therapeutic potential of DNase-based reperfusion strategy, Am. J. Physiol. Heart Circ. Physiol. 308 (5) (2015) H500–H509, https://doi.org/10.1152/ajpheart.00381.2014.
[61] G.A. Ramirez, M.R. Yacoub, M. Ripa, et al., Eosinophils from physiology to disease: a comprehensive review, BioMed Res. Int. 2018 (2018) 9095275, https://doi.org/10.1155/2018/9095275. Published 2018 Jan 28.
[62] C. Peet, A. Ivetic, D.I. Bromage, A.M. Shah, Cardiac monocytes and macrophages after myocardial infarction, Cardiovasc. Res. 116 (6) (2020) 1101–1112, https://doi.org/10.1093/cvr/cvz336.
[63] J. Liu, C. Yang, T. Liu, et al., Eosinophils improve cardiac function after myocardial infarction, Nat. Commun. 11 (1) (2020) 6396, https://doi.org/10.1038/s41467-020-19297-5. Published 2020 Dec 16.
[64] W. Li, H.M. Hsiao, R. Higashikubo, et al., Heart-resident CCR2+ macrophages promote neutrophil extravasation through TLR9/MyD88/CXCL5 signaling, JCI Insight 1 (12) (2016) e87315, https://doi.org/10.1172/jci.insight.87315.
[65] A.S. Jaggi, M. Singh, A. Sharma, D. Singh, N. Singh, Cardioprotective effects of mast cell modulators in ischemia-reperfusion-induced injury in rats, Methods Find Exp. Clin. Pharmacol. 29 (9) (2007) 593–600, https://doi.org/10.1358/mf.2007.29.9.1161005.
[66] S.A. Legere, I.D. Haidl, J.F. Légaré, J.S. Marshall, Mast cells in cardiac fibrosis: new insights suggest opportunities for intervention, Front. Immunol. 10 (2019) 580, https://doi.org/10.3389/fimmu.2019.00580. Published 2019 Mar 28.
[67] J.G. Rurik, H. Aghajanian, J.A. Epstein, Immune cells and immunotherapy for cardiac injury and repair, Circ. Res. 128 (11) (2021) 1766–1779, https://doi.org/10.1161/CIRCRESAHA.121.318005.